

## Peeling Mode Stability Studies of ELMs in ASDEX Upgrade

S. Saarelma<sup>1</sup>, S. Günter<sup>2</sup>, T. Kurki-Suonio<sup>1</sup>, M. Maraschek<sup>2</sup>, A.

Turnbull<sup>3</sup>, and H. Zehrfeld<sup>2</sup>

<sup>1</sup>*Helsinki University of Technology, Euratom-TEKES Association, FIN-02015 HUT, Finland*

<sup>2</sup>*Max-Planck-Institut für Plasmaphysik, Boltzmannstraße 2, D-85748 Garching bei München, Germany*

<sup>3</sup>*General Atomics inc., San Diego, CA 92138, USA*

A careful ELMy ASDEX Upgrade plasma equilibrium reconstruction is done taking into account the bootstrap current. The stability of the equilibrium is numerically analyzed using GATO [1] code and it is found that bootstrap current can drive plasma peeling mode unstable. This is one possible explanation for the ELM phenomenon.

### Introduction

ELMs (Edge Localized Modes) are short expulsions of the edge plasma. They are observed in the H-mode (High confinement) plasmas. Since operating in the H-mode is very important in the future reactors, the understanding of the ELMs is essential. However, the phenomenon still lacks a physical explanation.

Since the ELMs occur at the edge, an accurate reconstruction of the plasma equilibrium at the edge is important. While small in the core plasma, the bootstrap current is significant at the edge. Especially in the H-mode where steep gradients exist near the separatrix, the bootstrap current cannot be ignored in the equilibrium reconstruction.

In this paper, the role of the bootstrap current on the plasma stability is investigated and a proposed model for the ELMs is tested in realistic geometry and with experimental plasma profiles. Also plasma shaping especially triangularity is studied as means to control the ELMs.

### Bootstrap Current in Equilibrium Calculations

A standard free-boundary, separatrix-defined equilibrium is determined as a solution of

$$R^2 \nabla \cdot \frac{\nabla \Psi}{R^2} = -2\pi \mu_0 R j_{\tau} \quad (1)$$

where  $\Psi$  is the poloidal flux and the toroidal component of the current density is given by

$$j_{\tau} = \frac{\mu_0}{4\pi R} \frac{dJ^2}{d\Psi} + 2\pi R \frac{dp}{d\Psi} \quad (2)$$

Here  $J$  is the poloidal current and  $p$  the plasma pressure.

The standard way of calculating a plasma equilibrium is to prescribe functions  $dJ^2/d\Psi$  and  $dp/d\Psi$  and to solve the Poisson problem (1). Usually, it is possible to obtain the function  $dp/d\Psi$  from the experiments, but the poloidal current function is not known. Therefore, some assumptions of the  $dJ^2/d\Psi$  term has to be made. If the bootstrap current can be ignored, the poloidal current profile is independent of the temperature and pressure

profiles. However, at the plasma edge, where the gradients and the bootstrap current are large, this assumption is not valid.

An equilibrium including bootstrap current can be solved from Eq. (1) by conceiving  $dJ^2/d\Psi$  as expressed by the flux surface average  $\langle \mathbf{j} \cdot \mathbf{B} \rangle$ . Starting from the definition magnetic field, Ampère's law, and Eq. (1), it is possible to derive an expression

$$\langle \mathbf{j} \cdot \mathbf{B} \rangle = \langle B^2 \rangle \frac{dJ}{d\Psi} + \mu_0 J \frac{dp}{d\Psi}, \quad \langle \mathbf{j} \cdot \mathbf{B} \rangle = \iint \mathbf{j} \cdot \mathbf{B} \frac{dS}{|\nabla V|}. \quad (3)$$

Here, the surface averaged magnetic field  $\langle B^2 \rangle$  and its components are

$$\langle B^2 \rangle = \mu_0(L_P J^2 + L_T I^2), \quad \langle B_T^2 \rangle = \mu_0 L_P J^2, \quad \langle B_p^2 \rangle = \mu_0 L_T I^2, \quad (4)$$

where  $I$  is the toroidal current, and  $L_P$  and  $L_T$  are the inductance coefficients

$$L_P \equiv \frac{\mu_0}{4\pi^2} \langle 1/R^2 \rangle, \quad L_T \equiv \frac{4\pi^2 \mu_0}{\langle |\nabla V|^2 / R^2 \rangle}. \quad (5)$$

Using (3) the expression  $dJ/d\Psi$  can be eliminated from the Eq. (2) and we obtain

$$j_T = 2\pi R \left\{ \frac{B_T^2}{\langle B^2 \rangle} \frac{\langle \mathbf{j} \cdot \mathbf{B} \rangle}{\mu_0 J} + \left( 1 - \frac{B_T^2}{\langle B^2 \rangle} \right) \frac{dp}{d\Psi} \right\}. \quad (6)$$

We have eliminated  $dJ/d\Psi$  from the expression for  $j_T$ . However, it still depends on  $J$  itself and in addition on the toroidal current  $I$ . They can be solved, if  $\langle \mathbf{j} \cdot \mathbf{B} \rangle / \mu_0 J$  is given. Taking the flux surface average of Eq. (1) and using Eq. (3), we can derive two ordinary differential equations for  $I$  and  $J$  reading

$$\frac{dI}{dV} = \frac{\langle B_T^2 \rangle}{\langle B^2 \rangle} \frac{\langle \mathbf{j} \cdot \mathbf{B} \rangle}{\mu_0 J} + \left( 1 - \frac{\langle B_T^2 \rangle}{\langle B^2 \rangle} \right) \frac{dp}{d\Psi} \quad (7)$$

$$\frac{1}{2} \frac{dJ^2}{dV} = L_R I \frac{\langle B_T^2 \rangle}{\langle B^2 \rangle} \left\{ -\frac{\langle \mathbf{j} \cdot \mathbf{B} \rangle}{\mu_0 J} + \frac{dp}{d\Psi} \right\}. \quad (8)$$

Here  $L_R$  is a ratio of inductances  $L_T/L_P$

Considering now the functions  $\langle \mathbf{j} \cdot \mathbf{B} \rangle / \mu_0 J$  and  $dp/d\Psi$  as given and understanding  $\langle B^2 \rangle$  as described by (4) the solution of the subsequent nonlinear two-point boundary value problem described by (7) and (8) leads to a complete determination of the right-hand side for the Poisson problem Eq. (1): We prescribe  $I = 0$  on the magnetic axis and  $J^2 = J_p^2$  at the plasma boundary and solve for  $I$  and  $J^2$ . The solution for  $J^2$  can be used for the calculation of the current density according to Eq. (2). If the total plasma current  $I_p$  is prescribed we have more boundary conditions than dependent variables and therefore need one additional free parameter  $C_s$  in  $\langle \mathbf{j} \cdot \mathbf{B} \rangle = \langle \mathbf{j} \cdot \mathbf{B} \rangle(C_s)$ . Then the system (7) and (8) can be augmented by

$$\frac{dC_s}{dV} = 0, \quad (9)$$

so that we now have 3 variables and 3 boundary conditions.

In order to get the plasma equilibrium, we now need to prescribe only the flux surface averaged parallel current and the pressure gradient instead of  $dJ^2/d\Psi$ . In addition to prescribing the inductively driven current  $\langle \mathbf{j} \cdot \mathbf{B} \rangle_{CD} / \mu_0 J$ , it is possible to derive an analytical expression for  $\langle \mathbf{j} \cdot \mathbf{B} \rangle_{bs} / \mu_0 J$  which depends only on the pressure and temperature gradients,

and, thus, can be obtained from the experiments. This makes the bootstrap current equilibrium reconstruction possible. Three models with slightly different assumptions on the geometry and the collisionality were considered (Hirshman model and Harris model in [2] and Wesson model in [3]). It was found that the differences between the results obtained using different models were small. Figure 1 shows poloidal current density peaking at the edge as the bootstrap fraction of the total current is increased.

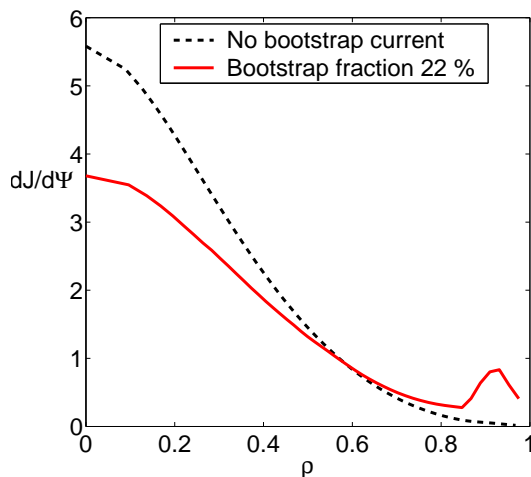


Figure 1: Poloidal current density distribution of an equilibrium with no bootstrap current (dashed line) and if the bootstrap current amounts 22 % of the total current (solid line).

## Bootstrap Current Driven Peeling Modes

Peeling modes are ideal kink modes that are localized at the plasma edge (Figure 2). An ASDEX Upgrade shot with type I ELMs (#11991) was analyzed using the GATO ideal MHD stability code. Temperature and density profiles were taken from the experiment and the bootstrap current was taken into account in the equilibrium reconstruction as described above. It was found that increasing the fraction of the bootstrap current from the total current caused plasma to become peeling mode unstable (Figure 3). Toroidal mode numbers ranging from 3 to 6 were found unstable. They agree with the Mirnov coil observations of the type I ELM precursors. Also, the calculated growth rates agree with the experimental observations of the MHD activity frequency prior to a type I ELM.

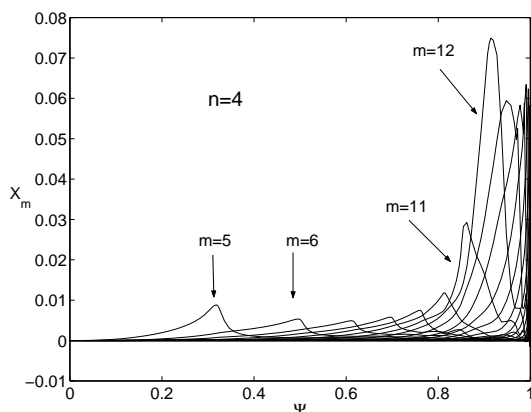


Figure 2: Fourier decomposition of a  $n=4$  peeling mode of the ASDEX Upgrade shot #11991 at 2.0 s

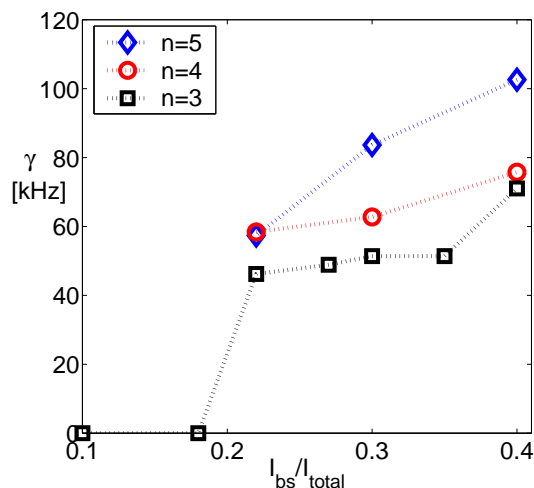


Figure 3: Peeling mode growth rates for three toroidal mode numbers. It can be seen that the growth rate of the instability increases as the bootstrap current is increased

## Triangularity

Two ASDEX Upgrade shots (#11991 and #11795) with similar plasma profiles but with differing plasma shapes were analyzed with respect to the peeling modes. It was found that increasing the plasma triangularity stabilizes the plasma (Figure 5). This is also supported by experimental observations. Long ELM-free periods have been detected in high triangularity shots but not with low triangularity. ELM frequencies are also lower in the high triangularity shots. Plasma shaping could be a method to control the ELMs.

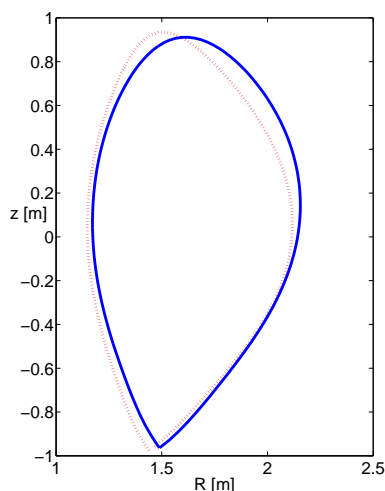


Figure 4: *Triangularity variation from  $\delta = 0.24$  (#11991, solid line) to  $\delta = 0.34$  (#11795, dotted line)*

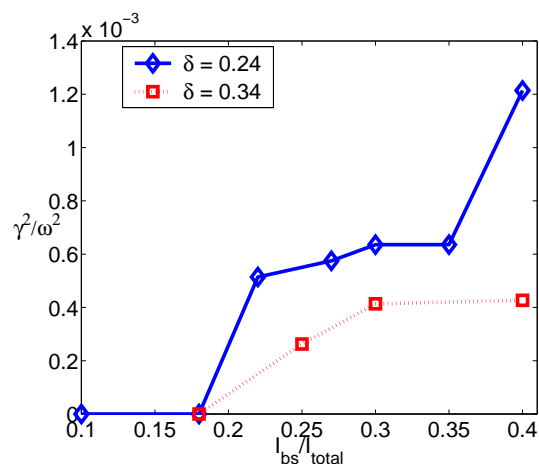


Figure 5: *Growth rates of the  $n=3$  peeling mode for medium ( $\delta = 0.24$ , solid) and high ( $\delta = 0.34$ , dotted) triangularity.*

## Discussion

Unstable peeling modes found in the equilibria with high bootstrap current fraction of the total current support the ELM model proposed in [4] for the limited circular plasmas. In this model, the ELM cycle starts with the development of the edge pressure pedestal. The pedestal starts increasing the bootstrap current and finally the bootstrap current destabilizes the plasma causing an ELM crash and the loss of the pedestal. In the light of the numerical results, it seems that the model is valid for diverted plasmas too.

## References

- [1] L. C. Bernard, F. J. Helton, R. W. Moore, Comp. Phys. Comm. 24 (1981) 377
- [2] C. Kessel, Nuclear Fusion, 34 (1994), 1221
- [3] J. Wesson, Tokamaks, 2nd ed. Clarendon Press, Oxford (1997)
- [4] J. W. Connor, R. J. Hastie, H. R. Wilson, MHD Stability of the Tokamak Edge, UKAEA FUS 383, 1997